



Transcriptomic and genomic changes associated with radioadaptation in *Exophiala dermatitidis*



Mackenzie E. Malo^{a,1}, Zachary Schultzhaus^{b,1}, Connor Frank^a, Jillian Romsdahl^c, Zheng Wang^{b,2}, Ekaterina Dadachova^{a,2,3,*}

^a University of Saskatchewan, College of Pharmacy and Nutrition, Saskatoon, Canada

^b Center for Biomolecular Science and Engineering, Naval Research Laboratory, Washington, DC, USA

^c National Research Council Postdoctoral Research Associate, Naval Research Laboratory, Washington, DC, USA

ARTICLE INFO

Article history:

Received 28 August 2020

Received in revised form 10 December 2020

Accepted 13 December 2020

Available online 19 December 2020

Keywords:

Fungi
Melanin
Ionizing radiation
Transcriptome
Radioadaptation

ABSTRACT

Melanized fungi have been isolated from some of the harshest radioactive environments, and their ability to thrive in these locations is in part due to the pigment melanin. Melanin imparts a selective advantage to fungi by providing a physical shield, a chemical shield, and possibly a signaling mechanism. In previous work we demonstrated that protracted exposure of the melanized yeast *Exophiala dermatitidis* to mixed alpha-, beta-, and gamma-emitting radiation resulted in an adapted strain able to mount a unique response to ionizing radiation in the environment in a melanin-dependent fashion. By exploring the genome and transcriptome of this adapted melanized strain relative to a non-irradiated control we determined the altered response was transcriptomic in nature, as whole genome sequencing revealed limited variation. Transcriptomic analysis indicated that of the adapted isolates analyzed, two lineages existed: one like the naïve, non-adapted strain, and one with a unique transcriptomic signature that exhibited downregulation of metabolic processes, and upregulation of translation-associated genes. Analysis of differential gene expression in the adapted strain showed an overlap in response between the control conditions and reactive oxygen species conditions, whereas exposure to an alpha particle source resulted in a robust downregulation of metabolic processes and upregulation of DNA replication and repair genes, and RNA metabolic processes. This suggest previous exposure to radiation primes the fungus to respond to subsequent exposures in a unique way. By exploring this unique response, we have expanded our knowledge of how melanized fungi interact with and respond to ionizing radiation in their environment.

© 2020 The Authors. Published by Elsevier B.V. on behalf of Research Network of Computational and Structural Biotechnology. This is an open access article under the CC BY-NC-ND license (<http://creativecommons.org/licenses/by-nc-nd/4.0/>).

1. Introduction

Numerous fungal species can be considered as some of the most radiation resistant organisms. They have been isolated from several extreme environments, such as Antarctic deserts, the Chernobyl Atomic Energy Station (including within reactor 4 where the disaster actually initiated), and the International Space Station (ISS) [37,46,35,34,44,4,5,43,20,12], and so have proven not only capable of surviving both acute and chronic exposure to various

forms of radiation whilst enduring a variety of other environmental stresses, but also thriving in these unique conditions [47].

In the search to identify what makes fungi so impervious to radiation, the pigment melanin has been identified as an interesting candidate. Melanin has been detected in ancient fossils dating back to the Cretaceous and Jurassic periods, and is present in most kingdoms, suggesting strong evolutionary preservation [55,31,16]. The presence of melanin, moreover, is associated with enhanced survival and improved fitness in extremely radioactive environments, as indicated by the prevalence of melanized fungal strains isolated from these locations [28]. This indicates that melanin has played an important role in Earth's history, and still imparts some important attributes to many organisms, particularly with regards to stress resistance.

In previous works, we and others have demonstrated that melanized fungal species, including *Cryptococcus neoformans*, *Exophiala*

* Corresponding author.

E-mail address: ekaterina.dadachova@usask.ca (E. Dadachova).

¹ These authors contributing equally to this work.

² These authors share senior authorship.

³ Corresponding Author

dermatitidis, and *Cryomyces antarcticus*, display enhanced growth and improved survival when exposed to ionizing radiation when compared to their non-melanized counterparts [29,30,27,36,11]. Melanin appears to enhance resistance to radioactive environments by providing a physical shield via Compton scattering, a chemical shield by quenching reactive oxygen species (ROS), altering growth kinetics and energy use, and possibly as a signaling mechanism by communicating conditions in the environment via its action as a redox capacitor, thereby initiating a transcriptomic response [11,10,50,7,19,25,41]. Work by Zhdanova and Tugay on fungal isolates from the Chernobyl “exclusion zone” demonstrated that a number of isolates were 1) resistant to, 2) stimulated by, and 3) adapted for growth in radioactive environments [49,12,48,56]. The fungal isolates demonstrated enhanced hyphal growth in the direction of a radioactive source, as well as enhanced spore germination, whereas control strains that had never been exposed to radiation experienced growth inhibition when exposed to radiation. The molecular details of how fungi detect, interact with, and respond to ionizing radiation in the environment, however, are unknown.

To investigate this issue further, we recently developed radiation adapted lab strains that could be used to further our understanding of this phenomenon [30] through the protracted exposure of melanized and non-melanized *E. dermatitidis* strains to Actinium-225 (^{225}Ac), which is a mixed alpha, beta and gamma-emitter. A subsequent phenotypic characterization of these “radioadapted” strains (Fig. 1) determined that the melanized, adapted strain showed increased colony size relative to naïve and albino control strains when grown adjacent to an alpha particle emitter, had enhanced electron transfer capacity, and displayed improved resistance to ROS. We interpreted these results to mean that previous exposure to ionizing radiation enhanced the capacity of our fungal cultures to detect and respond to radiation in the environment.

Our goal with the current study is to further understand the changes that occur in this adapted, melanized strain that enable it to detect and interact with ionizing radiation in the environment.

To that end, we set out to explore the genomic and transcriptomic landscape of several of these radioadapted strains. We found that, while few permanent mutations occurred during the adaptation process, one lineage of the melanized (wild type) adapted strain exhibited extensive transcriptomic changes, as well as the ability to respond to subsequent ionizing radiation exposure more robustly. Details of this response are provided below, which provide insight into how and why fungi grow and thrive in these uniquely harsh conditions.

2. Materials and methods

2.1. Growth conditions

The strains that were used in this experiment were the wild type (WT) strain of *E. dermatitidis* 8656 (aka ATCC34100, *Exophiala dermatitidis* CBS 525.76) and the albino mutant strain, *wdpks1* [14], that were either radioadapted by protracted exposure in media containing 1 mCi/ml ^{225}Ac or were passaged under background conditions and served as naïve controls, all of which were developed by our group in a previous study [30]. The protracted dose of 183 Gy/5 weeks delivered at a low dose rate of 0.02 mGy/min is a non-lethal dose for a melanized fungus, as melanized fungi can survive doses of >200 Gy delivered at high dose rates of >1000 mGy/min [28]. Single colonies from these naïve control and ^{225}Ac -adapted strains were isolated, cultured, and preserved as frozen glycerol stocks to be utilized for all experiments in this study (Table 1). Isolates were maintained in a modified Sabouraud

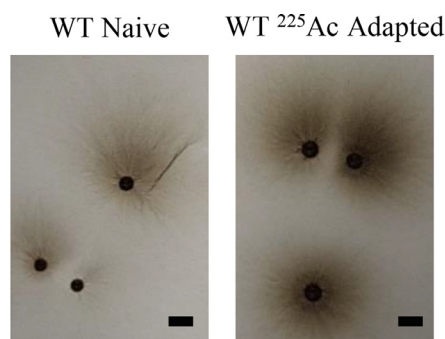


Fig. 1. Polonium-210 Exposure. Wildtype naïve (WTN) and wildtype ^{225}Ac adapted (WTA) *Exophiala dermatitidis* colonies growth adjacent to ^{210}Po source. Representative colonies shown with a 1 mm scale bar.

Table 1
Strains used in this study.

Original Strain	Adaptation conditions [30]	Total Dose (over 5 weeks/35d)	Isolate ID
ATCC34100, <i>Exophiala dermatitidis</i> CBS 525.76	Wildtype Naïve (WTN)	Background	1, 2
ATCC34100, <i>Exophiala dermatitidis</i> CBS 525.76	Wildtype ^{225}Ac Adapted (WTA)	183 Gy	3–6
<i>wdpks1</i>	Albino Naïve (<i>pksN</i>)	Background	7, 8
<i>wdpks1</i>	Albino ^{225}Ac Adapted (<i>pksA</i>)	183 Gy	9, 12

Emmons Broth (SAB; 2% dextrose, 1% peptone) at 30°C with shaking at 200 rpm until they reached an approximate concentration of 10^6 cells/ml. Cells were then transferred into minimal media (MM; 2 g/L KH_2PO_4 , 1.25 g/L $\text{MgSO}_4 \cdot 7\text{H}_2\text{O}$, 0.5 g/L glycine, 0.5 g/L dextrose, 0.003 g/L thiamine) and cultured at 30°C.

2.2. Polonium-210 exposure

Isolates grown in minimal media where dextrose was replaced with 0.01% sucrose (MMS) were used in alpha (α) particle radiation stimulation studies as previously described [30]. In brief, a 500 μCi Polonium-210 (^{210}Po) source (NRD, Grand Island, NY, USA) housed in a metal holder was placed within 3 mm of solid media. The source within the metal holder produced a collimated 0.5 $\mu\text{Gy/hr}$ beam of radiation that interacted with the solid growth media. Fungal cultures were diluted to a concentration of 10^3 cells/ml and approximately 10 cells were plated on solid MMS media such that they were outside of the collimated beam of radiation generated by the ^{210}Po source.

2.3. DNA and RNA sequencing

To obtain nucleic acids for genome and transcriptomic analysis, samples were prepared as follows. Isolate cultures were grown in MM as described above until the wildtype strains developed visible melanin, which was approximately 2 days, and were still in logarithmic growth. The concentration of each culture was measured and samples containing 3×10^7 cells/ml were collected through centrifugation, the supernatant removed, and the total genomic DNA extracted using OmniPrep™ for Yeast (G-Biosciences, St. Louis, MO).

For RNA collection, MM cultures of two wildtype naïve and four wildtype, melanized adapted strains were transferred to MMS and cultured for an additional 24 hrs to simulate starvation conditions.

Cultures were then adjusted to 10^7 cells/ml and transferred to 6-well plates. Each plate was then exposed to one of the following conditions:

- 1) Background radiation
- 2) Ionizing radiation exposure

The ^{210}Po strip (500 μCi) was placed directly above of the wells and generated a 0.5 $\mu\text{Gy/hr}$ dose rate. The fungi settled to the bottom, and the growth media was sufficient to shield alpha-particles from direct interaction with the fungal cells.

- 3) ROS exposure (through addition of 0.1 mM H_2O_2 to the medium)

Exposures took place at 30 °C in the dark for 1 week, after which total RNA was extracted from the samples with the RiboPure™ RNA purification Kit for Yeast (ThermoFisher Scientific). Libraries were constructed and sequenced on the Illumina NovaSeq S4 Sequencer by the Yale Center for Genome Analysis (YCGA, Yale School of Medicine, West Haven, CT).

2.4. Genomic analysis

For genome sequencing 2 wildtype naïve, 3 wildtype adapted, 2 *wdpks1* naïve, and 2 *wdpks1* adapted strains were analyzed (Table 1). The reference genome and annotation files for the raw paired-end 150 base reads were trimmed using Trimmomatic v 0.36 [6] and aligned to the publicly available *E. dermatitidis* NIH/UT8656 reference genome obtained from the EnsemblFungi web portal (<https://fungi.ensembl.org/>). Specifically, the Burrows-Wheeler Aligner (BWA) software package v 0.7.17 [24] was used to map reads and the sequence data was further processed using SAMtools v 1.9. PCR artifacts were removed using Picard tools MarkDuplicates (<https://broadinstitute.github.io/picard/>) and variants were identified using GATK v 3.8.7 [32]. GATK's IndelRealigner was used to realign reads containing putative INDELS and GATK's Haplotype Caller was used to call variants. GATK's Genotype GVCFs was used to combine the resulting Variant Call Format (VCF) files, which generated one VCF file for all *E. dermatitidis* WT samples and a second VCF files for *pks* samples, which were filtered using GATK's VariantFiltration based on stringent cutoffs for quality and coverage {SNPs: QD < 2.0, MQ < 40.0, QUAL < 100, FS > 60.0, MQRankSum < -12.5, SOR > 4.0, ReadPosRankSum < -8.0; INDELS: QD < 2.0, FS > 200.0, MQRankSum < -12.5, SOR > 4, InbreedingCoeff < -0.8, ReadPosRankSum < -20.0}. The resulting high-quality variants were then filtered such that any variant present in the naïve strain was removed from that strain's sample set. The remaining variants were annotated using annotation files obtained from EnsemblFungi and functional effects were predicted using snpEff [9].

2.5. Transcriptomic analysis

Analysis of RNA-seq data was performed on samples outlined in Table 2 in the following manner, as previously described [45]: transcript lengths and counts were determined using Salmon v. 1.3.0 software [38] with raw FASTQ reads as input and an index built from the *E. dermatitidis* NIH/8656 transcriptome that was assembled for prior experiments and is available on NCBI (Accession No. PRJNA224192) [45,8,41]. The resulting quant.sf files were used for pairwise comparisons with the DESeq2 package from Bioconductor version 3.0 [13] on R Studio version 3.1 [1]. Genes were differentially expressed between two conditions if their adjusted p-value (also referred to here as FDR) was <0.05. The resulting lists of differentially expressed genes were compared between conditions using Venny [33], and were analyzed for enrichment of certain Gene Ontology – Biological Process categories using FungiFun2 (<https://elbe.hki-jena.de/fungifun/>) [39].

Table 2
RNA Samples collected for Transcriptomic Analysis.

Condition	WT Melanized Strain Analyzed	Isolate ID
Background Radiation	WT Naïve Control (WTN-C)	1
		2
		3
		4
		5
		6
Ionizing Radiation Exposure (^{210}Po)	WT Naïve Radiation (WTN-R)	1
		2
		3
		4
		5
		6
Reactive Oxygen Species Exposure (H_2O_2)	WT Naïve Oxidation (WTN-O)	1
		2
		3
		4
		5
		6

3. Results and discussion

3.1. Genomic changes in radioadapted *E. dermatitidis* strains

Because ionizing radiation is a potent mutagen, we first assessed the genomic change that occurred within the adapted isolates from both the wildtype (WTA) and *wdpks1* (*pksA*) genetic backgrounds to understand how protracted exposure affected their DNA sequence.

An overview of the genetic variants identified in WTA and *pksA* strains relative to the naïve strains (WT and *pks*) are displayed in Table 3. Interestingly, very few mutations were observed in the WTA radioadapted strains, with the number of identified SNPs ranging from 0 to 2 and the number of INDELS ranging from 2 to 9. Observed variants included a missense mutation in strain WTA5 in the HMPREF1120_01028 gene, which encodes an ATP-dependent RNA helicase, a conservative inframe insertion in WTA3 in the HMPREF1120_07349 gene, which encodes a flagellar motor protein domain, and a disruptive inframe deletion in WTA6 in the HMPREF1120_00159 gene, which encodes a kinesin family member (Table 4, Supporting Table 1). Notably, two frameshift mutations (which often lead to a truncated or nonfunctional protein products) were observed in the WTA3 radioadapted strain. These variants occurred in stress-response nuclear envelope protein-encoding HMPREF1120_01736 and alpha/beta-hydrolase-encoding HMPREF1120_03360.

Among the *wdpks1*-radioadapted strains, *pksA9* featured 2 SNPs and 7 INDELS, which was comparable to the number of variants observed in the WT radioadapted strains (Table 3). These variants included frameshift mutations in HMPREF1120_06854, which encodes phytanoyl-CoA hydroxylase, and HMPREF1120_04304, which encodes ubiquitin-conjugating enzyme E2 (Table 5, Supporting Table 2). Notably, the latter frameshift insertion was also observed in *pksA12*. An increased number of SNPs was observed in *pksA12* relative to all other radioadapted strains (Table 5, Supporting Table 2). Most of these SNPs (17), and well as 2 INDELS, occurred in a 500 bp intergenic region approximately 2.5 kbs upstream from the coding region of HMPREF1120_04917, which encodes ubiquitin C-terminal hydrolase. The *pksA12* strain also harbored frameshift mutations that occurred in heat shock protein domain-encoding HMPREF1120_00517, arginase-encoding HMPREF1120_06649, and non-ribosomal peptide synthetase (NRPS) SidC-encoding HMPREF1120_07636, which is involved in siderophore biosynthesis. Another notable variant was an inter-

Table 3Summary of genetic mutations identified in WTA and *pksA* radioadapted strains relative to their respective naïve strain.

Strain ID	WTA3	WTA5	WTA6	<i>pksA9</i>	<i>pksA12</i>
No. of SNPs	0	2	1	2	21
Intergenic	0	1	1	1	19
Missense	0	1	0	0	2
UTR	0	0	0	1	0
No. of INDELS	9	2	3	7	12
Intergenic	5	2	2	5	5
Frameshift	2	0	0	2	4
UTR	1	0	0	0	1
Disruptive inframe	0	0	1	0	1
Conservative inframe	1	0	0	0	1
Total	9	4	4	9	33

Table 4

Genetic variants identified in WTA radioadapted strains relative to the WT naïve strain. The table describes the chromosome and nucleotide position of the variant, as well as the mutation type, which was predicted using snpEff. For intergenic variants, the gene name and annotation refer to the gene that is closest to that mutation.

CHROM	POSITION	MUTATION TYPE	GENE/NEAREST GENE	ANNOTATION	OCCURRENCE
1	433,055	Disruptive inframe deletion	HMPREF1120_00159	Kinesin family member	WTA6
1	2,836,819	Missense	HMPREF1120_01028	ATP-dependent RNA helicase	WTA5
2	631,490	Frameshift	HMPREF1120_01736	Stress-response nuclear envelope	WTA3
2	2,528,760	Intergenic	HMPREF1120_02387	UDP-glucose 4-epimerase	WTA3
3	1,006,101	Frameshift	HMPREF1120_03360	Alpha/beta-hydrolase	WTA3
3	1,268,882	3' UTR variant	HMPREF1120_03462	Phosphatidylinositol glycan	WTA3
3	1,576,609	Intergenic	HMPREF1120_03561	Alanine transaminase	WTA6
3	3,187,642	Intergenic	HMPREF1120_04157	MFS transporter	WTA3, WTA5, WTA6
4	1,158,832	Intergenic	HMPREF1120_04747	Carbonic anhydrase	WTA5
5	2,628,494	Intergenic	HMPREF1120_06504	SSS family solute:Na + symporter	WTA3, WTA6
6	1,418,001	Conservative inframe insertion	HMPREF1120_07349	Flagellar motor protein MotB domain	WTA3
6	1,971,753	Intergenic	HMPREF1120_07545	Redox-sensitive bicupin; pirin superfamily	WTA3, WTA5
7	1,180,436	Intergenic	HMPREF1120_08242	Hypothetical protein	WTA3

Table 5Genetic variants identified in *pksA* radioadapted strains relative to the *pks* naïve strain. The table describes the chromosome and nucleotide position of the variant, as well as the mutation type, which was predicted using snpEff. For intergenic variants, the gene name and annotation refer to the gene that is closest to that mutation.

CHROM	POSITION	MUTATION TYPE	GENE/NEAREST GENE	ANNOTATION	OCCURRENCE
1	1,426,160	Frameshift	HMPREF1120_00517	DnaJ-domain (heat shock protein)	<i>pksA12</i>
1	3,069,904	Intergenic	HMPREF1120_01094	DNA Pol 3 subunit	<i>pksA9</i> , <i>pksA12</i>
3	843,500	5' UTR variant	HMPREF1120_03304	Endo-1,3(4)-beta-glucanase	<i>pksA9</i>
3	2,568,652	3' UTR variant	HMPREF1120_03921	Hypothetical protein	<i>pksA12</i>
3	3,187,642	Intergenic	HMPREF1120_04157	MFS transporter	<i>pksA9</i> , <i>pksA12</i>
3	3,617,951	Frameshift	HMPREF1120_04304	Ubiquitin-conjugating enzyme E2	<i>pksA9</i> , <i>pksA12</i>
4	1,631,962	Intergenic	HMPREF1120_04917	Ubiquitin C-terminal hydrolase	<i>pksA12</i>
4	1,631,965	Intergenic	HMPREF1120_04917	Ubiquitin C-terminal hydrolase	<i>pksA12</i>
4	1631762–1632254	17 Intergenic variants	HMPREF1120_04917	Ubiquitin C-terminal hydrolase	<i>pksA12</i>
5	998,035	Conservative inframe deletion	HMPREF1120_05954	Transducin (beta)-like 1	<i>pksA12</i>
5	3,033,533	Frameshift	HMPREF1120_06649	Arginase	<i>pksA12</i>
6	48,768	Frameshift	HMPREF1120_06854	Phytanoyl-CoA hydroxylase	<i>pksA9</i>
6	1,198,245	Missense	HMPREF1120_07268	Alcohol dehydrogenase (NADP+)	<i>pksA12</i>
6	1,666,136	Disruptive inframe deletion	HMPREF1120_07440	MFS transporter, SP family, sugar:H + symporter	<i>pksA12</i>
6	1,971,753	Intergenic	HMPREF1120_07545	Redox-sensitive bicupin; pirin superfamily	<i>pksA9</i>
6	1,971,778	Intergenic	HMPREF1120_07545	Redox-sensitive bicupin; pirin superfamily	<i>pksA12</i>
6	2,002,737	Intergenic	HMPREF1120_07554	Hypothetical protein	<i>pksA9</i>
6	2,252,182	Frameshift	HMPREF1120_07636	NRPS SidC (siderophore biosynthesis)	<i>pksA12</i>
7	70,963	Intergenic	HMPREF1120_07867	Multi-sensor signal transduction histidine kinase	<i>pksA12</i>
7	1,099,400	Intergenic	HMPREF1120_08213	Transcription factor	<i>pksA9</i>
7	1,142,537	Missense	HMPREF1120_08228	Hypothetical protein	<i>pksA12</i>
7	1,503,364	Intergenic	HMPREF1120_08366	Autophagy-related protein	<i>pksA9</i> , <i>pksA12</i>

genic SNP, identified in 2 WTA and both *pksA* radioadapted strains, that was approximately 1.4 kbps away from HMPREF1120_07545, which encodes a protein with similarity to redox-sensitive bicupin YhaK.

3.2. Transcriptomic characterization of radioadapted *E. dermatitidis*

We previously demonstrated that radioadaptation resulted in the increased colony growth in radioadapted strains in comparison with naïve strains when both strains were exposed to ionizing

radiation from an α particle emitting Polonium-210 source, as well as increased electron transfer capacity, and improved resistance to the toxic effects of ROS [30].

To understand what was occurring to produce this altered biological response, we set out to characterize the transcriptome of the adapted, melanized strain (WTA) relative to the naïve, melanized strain (WT). For this experiment, we used wild type strains (Table 2) that were also characterized by genome sequencing, including four strains isolated from the wildtype ²²⁵Ac adapted culture (WTA3-6) were used, along with two control strains

(WTN1-2) that were isolated from a naïve, wildtype culture not previously exposed to this radionuclide. We did not perform this analysis on the non-melanized strains, as they did not exhibit radiation-associated phenotypes in our initial experiments [30].

The overall transcript reads and expression changes between each strain and condition are given in Supporting Tables 3 and 4. The first analysis on this data that we performed on this data was to view the correlation between Transcripts Per Million (TPM) values produced by the Salmon alignment and transcript quantification program, to determine how each dataset was correlated across replicates, strains, and conditions. Notably, Fig. 2 shows that this comparison revealed that the TPM values from control sample 1 (wildtype, naïve sample 1C) highly correlated ($R^2 > 0.95$) not only with sample 2 (wildtype, naïve sample 2C), but with also samples 3 (wildtype, adapted 3C) and 6 (wild type, adapted 6C), whereas samples 4 (wildtype, adapted 4C) and 5 (wildtype, adapted 5C) were closely correlated with each other under this condition ($R^2 = 0.9735$) but substantially different than the other four samples ($R^2 < 0.73$). This suggested to us that the adapted culture from which the four strains were isolated included a mixture of at least two strains – one with a transcriptome that we observed was similar to the naïve strain, and one that had a unique transcriptomic signature. The second observation we made from this analysis, as demonstrated in Fig. 3, was that the subsequent stress exposures (to ^{210}Po and H_2O_2) had extremely minor effects on the transcriptomes of both sets of strains (represented here by WT1 and WTA4). Overall, the number of differentially expressed genes between each condition and sample can be observed in Fig. 4.

3.3. Differentially expressed genes in the adapted strains

It is clear from the total number of differentially transcribed genes, that the major differences observed were associated with the adaptation process in isolates 4 and 5, and not the exposure conditions. These strains demonstrated that, although not essential, there was a possibility for a marked change in gene expression in cells that were incubated in such an environment, so we focused on the differences between these (hereafter WTA) and the naïve (hereafter WTN) strains. We did this by analyzing the transcripts that changed in abundance between these two pairs of strains either in background conditions or after exposure to ^{210}Po or to 0.1 mM H_2O_2 under conditions of starvation. Such differences under background conditions would suggest more stable changes between the two strains that could potentially be used as signatures of previous exposure in *E. dermatitidis*, while differences in the response to ^{210}Po , for example, would reflect the responses of radioadapted strains to future radiation challenge. Fig. 5 attempts to unravel these possibilities by observing the overlap between these three sets of up- and down-regulated genes. Interestingly, although the exposure did not greatly affect the transcriptome in any given strain lineage, less than half of the differentially expressed genes were shared among the three conditions, suggesting that the adapted strains had a unique response to these distinct environments. This was especially notable for ^{210}Po exposure, as 696/1713 of the genes differentially expressed between the two strains were unique to this condition. We view this result as evidence that the adapted strain had the ability to respond more robustly to a second exposure to ionizing radiation.

The differences between the WTN and WTA strains with varied transcriptomic signatures become even clearer after gene enrichment analysis, where one considers the function of these sets of significantly regulated transcripts (Table 6). We observed that in all cases, genes encoding proteins involved in oxidation–reduction processes were significantly downregulated in the adapted compared to the naïve. The oxidation–reduction process title is some-

what misleading, as what we actually see are genes involved in catalyzing redox reactions in the context of the electron transport chain and metabolism (Supporting Table 8), and include enzymes such as alcohol dehydrogenase, acyl-CoA dehydrogenase, cytochrome P450 monooxygenase, glucose-1 dehydrogenase [17]. When you look at how the genes in this process overlap, a substantial number were unique to the radioactive environment conditions (Fig. 5 and Supporting Tables 5–7), yet these unique genes were still primarily involved in catalyzing redox reactions in the context of the electron transport chain and metabolism. There is a down regulation in catalase (HMPREF1120_07713) and superoxide dismutase (HMPREF1120_05007,) which are enzymes involved in response to oxidative stress [54] but they are downregulated in the adapted strains across all conditions. This suggest that it is part of the adaptive process, but not involved in the mechanisms involved in improved fitness and ROS resistance observed under subsequent exposure to radiation.

Transmembrane transport and the general category of “metabolic process” were also downregulated in two out of the three gene sets. These are relatively vague functional classes, but overall, they suggest a suppression down of several primary metabolic and redox reactions in the adapted strains.

The patterns observed in the upregulated group were easier to interpret. For example, functions related to translation were enriched in all three sets. This suggests an increase in protein production, which was, interestingly, also observed when *E. dermatitidis* was grown in the presence of low dose γ -radiation [41]. Another interesting observation is the enrichment of genes involved in DNA replication in the adapted cells exposed to ^{210}Po , a pattern which was even clearer when only the genes unique to this condition were analyzed (Fig. 5). In this case, not only DNA replication but DNA recombination was enriched, as well as the obsolete ATP catabolic processes, which upon review included 27 genes, including 13 helicases, 2 DNA topoisomerases, and an elongation factor (EF-3), many of which are involved in RNA remodeling, DNA repair, [21,2,15,3]. Overall, there were many genes that were unique between the WTR and the AR set compared to the two other conditions (Supporting Tables 5–7). This points to both the possible presence of DNA damage even under these low dose conditions as well as the ability of the adapted strain to respond more quickly and robustly to such damage. Genes uniquely upregulated in the adapted strain in response to irradiation included several DNA helicases, DNA ligase, and the DNA repair proteins rad52, ERCC-6, rhp54, rad9, uvsE, among others, while downregulated genes, which showed a greater magnitude of regulation, included transporters (10 major facilitator superfamily proteins), but mostly included proteins with only general predictions, suggesting that this regulatory response was subtle and complex, and involved in several biosynthetic pathways (e.g. biotin and glycogen synthesis, Supporting Tables 5 and 7). In all, although we did not observe large responses to exposure to oxidative stress or irradiation, we did observe a strong and consistent change in one lineage of *E. dermatitidis* that was adapted to long-term radionuclide presence, and we observed evidence that this adaptation process allowed for this strain to become more responsive to future ionizing radiation exposure.

3.4. Adaptation in *E. dermatitidis*

The purpose of the study was to identify the underlying genomic and transcriptomic events that are the result of radioadaptation in *E. dermatitidis* cultures and to further understand how those changes impact the fungal response to subsequent radiation exposure. These changes, we believe, would allow us to identify and understand the adaptation that is taking place.

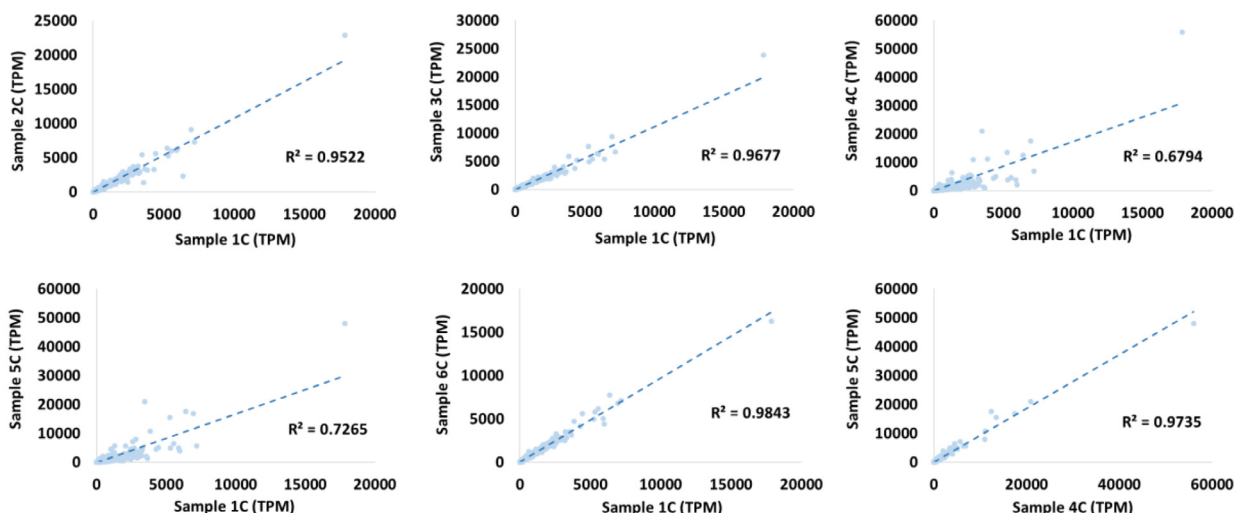


Fig. 2. Comparison of control RNAseq samples using Transcripts Per Million (TPM) values observed for each predicted transcript encoded by the *E. dermatitidis* genome. Samples 1 and 2 represent naïve strains, while samples 3–6 represent adapted strains.

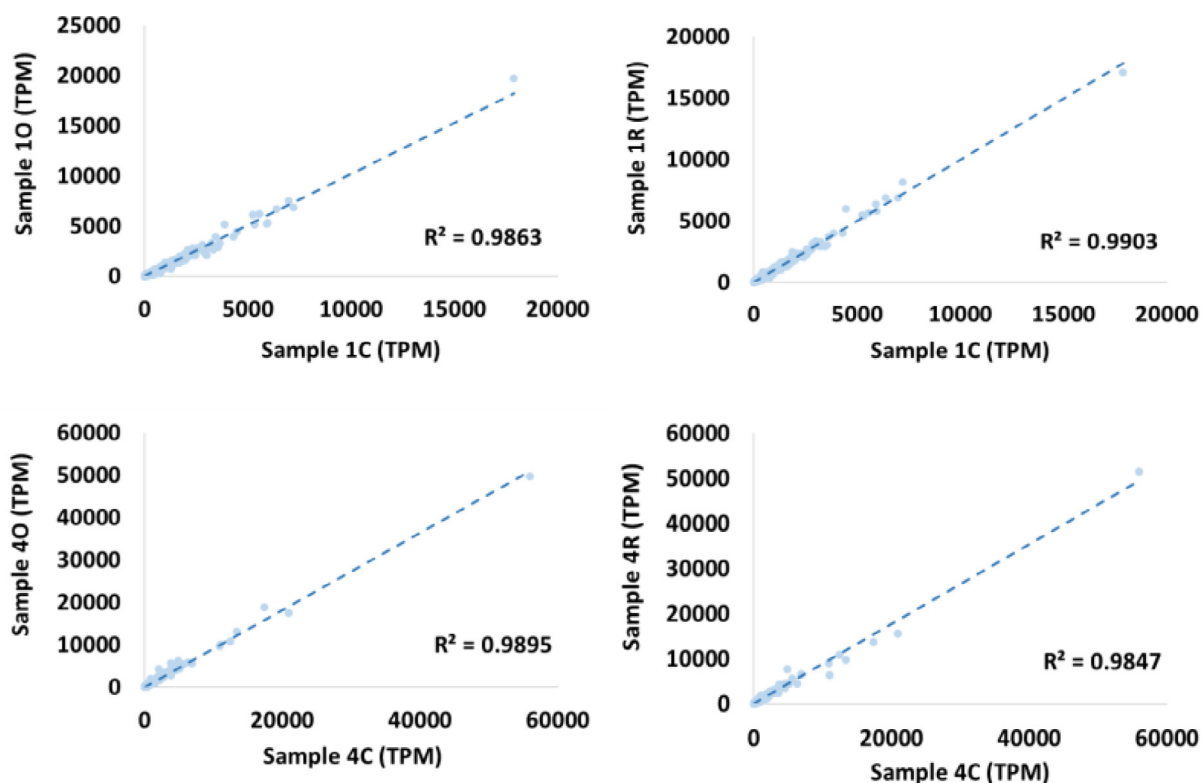


Fig. 3. Comparison of the responses of naïve (Strain 1) and adapted (Strain 4) to H₂O₂ (O) and Polonium-210 (R) exposure, visualized with RNAseq data using Transcripts Per Million (TPM) values observed for each predicted transcript encoded by the *E. dermatitidis* genome.

Ionizing radiation induces the production of free radicals, including reactive oxygen and nitrogen species. Our previous data demonstrated that radioadapted cells presented similar biological responses to both subsequent H₂O₂ and ionizing radiation exposure, so we could not determine whether adapted strains could distinguish these stresses [30]. In our previous work we assessed response of the adapted strains to strontium-90 (beta) and cesium-137 (gamma) [30]. We found that while there was a stimulation of growth with a gamma emitter in the naïve strain, the adapted strain showed no enhanced growth. Neither the naïve

nor the adapted strain showed enhanced growth with a beta source.

Here, what we observed was enhanced colony growth in our melanized adapted strain (Fig. 1) only when using ²¹⁰Po, an alpha-particle emitter. Relative to gamma and beta radiation, alpha particles have with a high linear energy transfer (LET) and are capable of generating more ROS through radiolysis when interacting with the growth media that the fungus would be plated on [22]. This is why alpha radiation is densely-ionizing, while gamma and beta radiation are sparsely-ionizing. We did not observe any

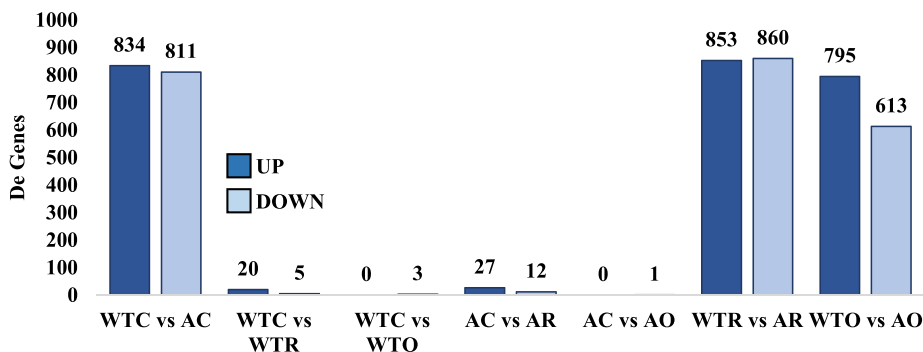


Fig. 4. RNA-seq results demonstrated as the total number of differentially expressed (DE) genes (FDR < 0.05) between pairwise comparisons of samples and conditions in this experiment. Strains include wildtype (WT) and adapted (A). Conditions include background (C), H₂O₂ (O), or ionizing radiation (R).

enhanced growth response when these strains were grown near radioactive sources with lower LET, so we hypothesized that the difference in biological response could be due to enhanced resistance to the toxic effects of the ROS generated by the alpha particles. This hypothesis seemed plausible, as our melanized adapted strain presented enhanced resistance to H₂O₂.

Our initial analysis using whole genome sequencing was completed to compare the naïve and adapted strains of the melanized wildtype and albino *wdpks1* mutants (Table 1). There was not a significant difference in the number or type of mutations when comparing the adapted strains of the WTA to the *pksA* mutants (Table 3–5) which indicates the phenotypic changes observed in the melanized adapted strain were not genomic in nature. In fact, only 4 mutations were observed in the one of the strains that presented an altered transcriptomic signature (Table 5).

The transcriptomic analysis, unsurprisingly, provided us with more information to explore. With this data, we were able to make two major conclusions. First, we observed that the stresses that we challenged these strains with (²¹⁰Po and H₂O₂) did not dramatically affect the transcriptome, at least at the time point that we characterized (1 week). This suggests that *E. dermatitidis* can return its transcriptome to a steady state after an extended period under a moderate stress. Second, we identified two lineages with varied transcriptomic signatures in the radioadapted, melanized *E. dermatitidis* strain. One lineage aligned with the naïve strain (Figs. 2 and 3), while the other presented a unique signature. It is not surprising that we observed different lineages within the adapted strain, as adaptation was performed on a pool of stationary phase cells where individual cells would have gone through radiation and age-related mutagenesis, which would have resulted in some variance [18,42].

We then focused on the lineage that showed a distinct expression pattern, which provided us with several interesting results. First, we observed a general upregulation of translation genes, which could suggest that the adapted strains enhance their protein synthesis machinery for resilience to environmental stresses, such as ionizing radiation and ROS. We previously observed a similar expression pattern upon low dose gamma irradiation in wildtype *E. dermatitidis* [41] while in response to acute, high dose gamma irradiation we see the opposite pattern – ribosomal genes being strongly downregulated [45]. Ribosomal biosynthesis is tightly associated with growth rate, so the upregulation of this set of genes may be a mark of the apparent increase in growth rate we observe in the adapted strains [53]. The enrichment of genes involved in glycolysis (glycolytic process) among the upregulated transcripts in the adapted strains may also be indicative of faster growth. On the other hand, several genes in the GO categories of oxidation–reduction processes and metabolic processes were significantly downregulated. We consider this to signify two potential

situations. First, because these enzymes were generally involved in a wide variety of diverse and vague metabolic pathways, it is possible that their downregulation is due to an overall streamlining of the cell toward protein synthesis. Second, these changes could indicate an overall global change in the redox balance of the cell, which is to be expected in strains adapted to high ROS environments such as chronic irradiation. Electron transport and metabolism, in fact, themselves are a source of ROS [17,54] so a down regulation in these processes could reduce the internal production of ROS, and thereby position the fungi to withstand a more robust external load of ROS. Respiration in fungi is not a linear process but is in fact significantly branched, with numerous alternative enzymes [17]. The more substantial response in downregulation of more of these enzymes in the ²¹⁰Po conditions (Fig. 5B) thereby reducing the redundancy in the metabolic processes and could be a unique response to the ²¹⁰Po conditions to further reduce the internal ROS load.

Finally, by comparing the pairwise analysis of wild type and adapted strains responding to each condition, another subset of genes, specifically upregulated in response to ²¹⁰Po exposure was revealed. These included genes traditionally associated with ionizing radiation damage, including those involved in DNA replication and recombination. This finding is interesting considering the extensive literature on “inducible repair” in fungi, where cells recovering from an initial exposure to ionizing radiation are more resilient to a subsequent exposure [23,51]. This is presumably due to the cell’s ability to mount and therefore more efficiently respond to the second round of damage, but this phenomenon has not generally been characterized at the transcriptomic level. It is also particularly interesting because this response is distinct from the response to H₂O₂, suggesting that the cellular responses to general oxidative stress do not necessarily overlap with the response to ionizing radiation exposure. It will be interesting, at this juncture, to understand whether these changes result in increased resistance to acute ionizing radiation or other DNA damage [52] as it is still controversial whether the inducible repair response is mediated at the transcript or protein level, and most experiments on inducible repair do not initiate with exposure to the low doses that were used with these adapted strains.

In our previous work melanized *E. dermatitidis* presented an altered biological response following the adaptation process in the face of subsequent radiation and ROS exposures while the non-melanized strain did not [30]. This observation led us to hypothesize that we would observe a robust transcriptomic response under these same conditions in the melanin biosynthetic pathway, represented by the polyketide synthase (PKS) gene (HMPREP1120_03173). Analysis of the transcriptome of the adapted strains showed a slight down regulation of the PKS gene under all conditions when compared to the naïve strain (Support-

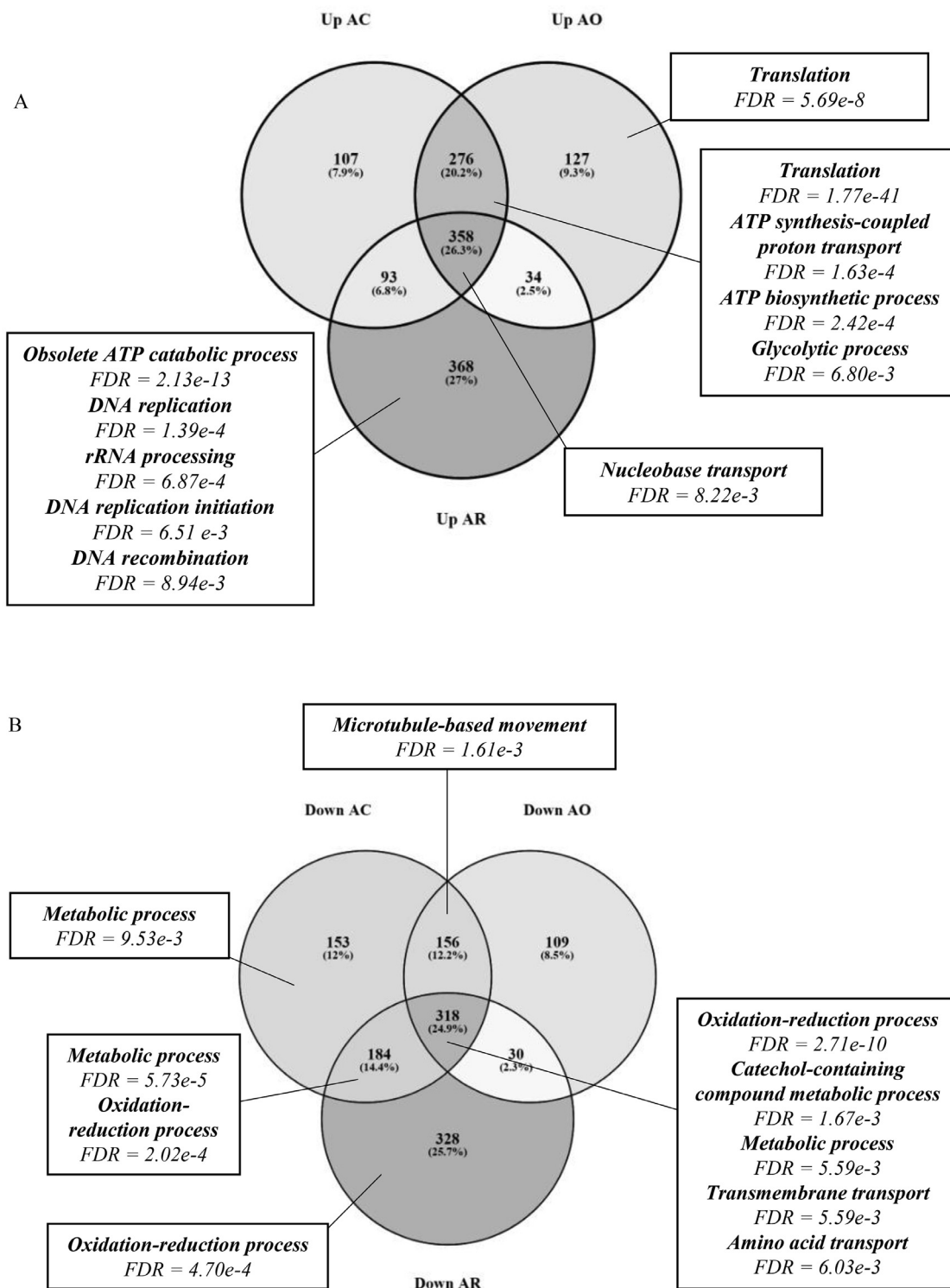


Fig. 5. Venn diagram demonstrating the number of differentially expressed genes (FDR < 0.05) that are either upregulated (left) or downregulated (right) in the adapted strains relative to the wild type strains when exposed to background (C), H₂O₂ (O), or ionizing radiation (R). Gene Ontology – Biological Processes as provided by Fungifun (see Methods). Percentages indicate fraction of total differentially expressed genes.

ing Table 4) with log2fold change values ranging from −0.49 to −0.63. While melanin plays an essential role in the phenotypic response of adapted *E. dermatitidis*, transcriptomic regulation of the biosynthesis of the pigment does not appear to be substantially altered by the adaptation process. We also looked at alterations in carotenoid genes (HMPREF1120_03263, HMPREF1120_02864), which are known for their antioxidant and photoprotective

properties [26,40] and found no substantial changes (Supporting Table 4) due to the adaptation process in these genes.

4. Conclusion

In conclusion, we observed several things when completing a genomic and transcriptomic study on *E. Dermatitidis* strains

Table 6

Gene Ontology categories (Biological process) that were determined to be significantly enriched (FDR < 0.01) among the genes that were differentially expressed (FDR < 0.05) between naïve and adapted strains under each condition, as determined using FungiFun.

	GO term classification (Biological Process)	Adjusted p-value	# genes/category	# genes/input
Down in WTA-C vs WTN-C	oxidation–reduction process	4.60e-18	165/832	165/811
	metabolic process	1.76e-09	183/1175	183/811
	transmembrane transport	1.14e-04	77/459	77/811
Up in WTA-C vs WTN-C	translation	1.26e-20	62/150	62/834
	glycolytic process	3.27e-04	10/18	10/834
	cellular amino acid biosynthetic process	6.18e-04	12/27	12/834
Down in WTA-O vs WTN-O	oxidation–reduction process	7.66e-11	119/832	119/613
	transmembrane transport	2.74e-04	61/459	61/613
	microtubule-based movement	3.87e-03	6/13	6/613
	catechol-containing compound metabolic process	7.09e-03	3/3	3/613
Up in WTA-O vs WTN-O	translation	5.83e-36	76/150	76/795
	ATP synthesis coupled proton transport	1.13e-03	8/14	8/795
	glycolytic process	1.18e-03	9/18	9/795
Down in WTA-R vs WTN-R	Oxidation-reduction process	1.88e-20	179/832	179/860
	metabolic process	2.35e-08	189/1175	189/860
Up in WTA-R vs WTN-R	DNA replication initiation	2.39e-03	6/8	6/853
	DNA replication	5.30e-03	14/44	14/853
	formation of translation preinitiation complex	5.30e-03	7/13	7/853
	regulation of translational initiation	5.30e-03	7/13	7/853
	ribosome biogenesis	9.27e-03	10/27	10/853

adapted to ²²⁵Ac exposure. First, the adaptation response appeared to be mediated at the transcriptomic level, as the adaptation process resulted in very few, and likely insubstantial genetic mutations. This also supports the extremely stable genome in the face of protracted exposure to ionizing radiation. Second, we found that even a low dose of radiation with a high LET in the environment, or ROS in the form of H₂O₂, elicited a transcriptomic response that in general resulted in down regulation of metabolic transcripts and an up regulation in translation in the adapted versus naïve melanized *E. dermatitidis*. Downregulation of metabolic processes in general would reduce the internal ROS load, thereby positioning the adapted fungi to better respond to an external load of ROS, while an upregulation of translation would prime the fungi for growth. Finally, we noted, that despite a similar number of up/down regulated transcripts, the adapted cultures, when exposed to radiation in their environment, presented a unique transcriptomic profile, whereas the transcriptomic profile of the culture exposed to ROS significantly overlapped with the control culture. While several of the differentially regulated processes were similar between the conditions, the scale of transcripts that were unique to the ²¹⁰Po condition suggests a more robust response. Also unique to this condition was a general upregulation of DNA replication and repair enzymes, suggesting that previous exposure to radiation positions the adapted strain to better respond to damage caused by an alpha-particle emitting source in its environment. From this we can conclude that the adaptation process resulted in an altered transcriptomic response from fungus grown in the same conditions without radiation, and that this previous exposure altered how this fungus responded to subsequent interactions, even indirect.

Funding information

The work was funded by the Defense Threat Reduction Agency grant HDTRA-17-1-0020.

CRediT authorship contribution statement

Mackenzie E. Malo: Conceptualization, Data curation, Formal analysis, Investigation, Methodology, Project administration, Validation, Visualization, Writing – original draft, Writing – review & editing. **Zachary Schultzhaus:** Data curation, Formal analysis, Writing – original draft, Writing – review & editing. **Connor Frank:**

Investigation. **Jillian Romsdahl:** Data curation, Formal analysis, Writing – original draft, Writing – review & editing. **Zheng Wang:** Funding acquisition, Supervision, Writing – review & editing. **Eka-terina Dadachova:** Funding acquisition, Project administration, Resources, Supervision, Writing – review & editing.

Appendix A. Supplementary data

Supplemental Table 1: SNPs and INDELS identified in WTA radioadapted strains. Supplemental Table 2: SNPs and INDELS identified in *pksA* radioadapted strains. Supplemental Table 3: Salmon output for analysis of transcriptomic data including transcripts per million (TPM) and transcript read lengths. Supplemental Table 4: Output from DEseq2 analysis between given conditions demonstrating Log2fold changes and significance information. Genes with a padj < 0.05 were determined to be differentially expressed. Supplemental Table 5: Genes that were uniquely upregulated/downregulated in adapted strains compared to naïve strains, in the presence of ionizing radiation. Supplemental Table 6: Uniprot annotations of upregulated genes from Supplemental Table 5. Supplemental Table 7: Uniprot annotations of downregulated genes from Supplemental Table 5. Supplemental Table 8: Enriched genes in the GO:005514 Oxidation-Reduction Process category. Supplementary data to this article can be found online at <https://doi.org/10.1016/j.csbj.2020.12.013>.

References

- [1] J. Allaire, RStudio: Integrated Development Environment for R. ed. R. Team". Boston, MA 770, 2012.
- [2] Arenas JE, Abelson JN. Prp43: An RNA helicase-like factor involved in spliceosome disassembly. *Proc Natl Acad Sci USA* 1997;94(22):11798–802.
- [3] Bernstein KA, Gangloff S, Rothstein R. The RecQ DNA helicases in DNA repair. *Annu Rev Genet* 2010;44(1):393–417.
- [4] Blachowicz A, Chiang AJ, Elsaesser A, Kalkum M, Ehrenfreund P, Stajich JE, Torok T, Wang CCC, Venkateswaran K. Proteomic and metabolomic characteristics of extremophilic fungi under simulated mars conditions. *Front Microbiol* 2019;10:1013.
- [5] Blachowicz A, Chiang AJ, Romsdahl J, Kalkum M, Wang CCC, Venkateswaran K. Proteomic characterization of *Aspergillus fumigatus* isolated from air and surfaces of the International Space Station. *Fungal Genet Biol* 2019;124:39–46.
- [6] Bolger AM, Lohse M, Usadel B. Trimmomatic: a flexible trimmer for Illumina sequence data. *Bioinformatics* 2014;30:2114–20.
- [7] Bryan R, Jiang Z, Friedman M, Dadachova E. The effects of gamma radiation, UV and visible light on ATP levels in yeast cells depend on cellular melanization. *Fungal Biol* 2011;115(10):945–9.
- [8] Chen Z, Martinez DA, Gujja S, Sykes SM, Zeng Q, Szanislo PJ, et al. Comparative genomic and transcriptomic analysis of *wangiella dermatitidis*, a major cause

- of phaeohyphomycosis and a model black yeast human pathogen. *G3* (Bethesda Md) 2014;4(10):561–78.
- [9] Cingolani P, Platts A, Wang LL, Coon M, Nguyen T, Wang L, et al. A program for annotating and predicting the effects of single nucleotide polymorphisms, SnpEff: SNPs in the genome of *Drosophila melanogaster* strain w1118; iso-2; iso-3. *Fly* 2012;6(2):80–92.
- [10] Dadachova E, Bryan RA, Howell RC, Schweitzer AD, Aisen P, Nosanchuk JD, Casadevall A. The radioprotective properties of fungal melanin are a function of its chemical composition, stable radical presence and spatial arrangement. *Pigment Cell Melanoma Res* 2008;21:192–9.
- [11] Dadachova E, Bryan RA, Huang X, Moadel T, Schweitzer AD, Aisen P, Nosanchuk JD, Casadevall A. Ionizing radiation changes the electronic properties of melanin and enhances the growth of melanized fungi. *PLoS One* 2007;2.
- [12] Dighton J, Tugay T, Zhdanova N. Fungi and ionizing radiation from radionuclides. *FEMS Microbiol Lett* 2008;281:109–20.
- [13] Doerge RW. *Bioinformatics and Computational Biology Solutions Using R and Bioconductor* Edited by Gentleman, R., Carey, V., Huber, W., Irizarry, R., and Dudoit. *S Biometrics* 2006;62:1270–1.
- [14] Kozel TR, Feng B, Wang Xu, Hauser M, Kaufmann S, Jentsch S, et al. Molecular cloning and characterization of WdPKS1, a gene involved in dihydroxynaphthalene melanin biosynthesis and virulence in *Wangiella* (*Exophiala*) dermatitidis. *Infect Immun* 2001;69(3):1781–94.
- [15] Gilman B, Tijerina P, Russell R. Distinct RNA-unwinding mechanisms of DEAD-box and DEAH-box RNA helicase proteins in remodeling structured RNAs and RNPs. *Biochem Soc Trans* 2017;45:1313–21.
- [16] Glass K, Ito S, Wilby PR, Sota T, Nakamura A, Bowers CR, et al. Direct chemical evidence for eumelanin pigment from the Jurassic period. *Proc Natl Acad Sci* 2012;109(26):10218–23.
- [17] T. Joseph-Horne, D.W. Hollomon, P.M. Wood, Fungal respiration: a fusion of standard and alternative components. *Biochim. Biophys. Acta (BBA) – Bioenergetics*, 1504 (2001), 179–195.
- [18] Kaya A, Lobanov AV, Gladyshev VN. Evidence that mutation accumulation does not cause aging in *Saccharomyces cerevisiae*. *Aging Cell* 2015;14(3):366–71.
- [19] Kim E, Kang M, Tschirhart T, Malo M, Dadachova E, Cao G, et al. Spectroelectrochemical reverse engineering demonstrates that Melanin's redox and radical scavenging activities are linked. *Biomacromolecules* 2017;18(12):4084–98.
- [20] Knox BP, Blachowicz A, Palmer JM, Romsdahl J, Huttenlocher A, Wang CCC, et al. Characterization of *Aspergillus fumigatus* isolates from air and surfaces of the international space station. *mSphere* 2016;1(5).
- [21] Kressler D, de la Cruz J, Rojo M, Linder P. Fal1p is an essential DEAD-box protein involved in 40S-ribosomal-subunit biogenesis in *Saccharomyces cerevisiae*. *Mol Cell Biol* 1997;17(12):7283–94.
- [22] Le Caër S. Water radiolysis: influence of oxide surfaces on H₂ production under ionizing radiation. *Water* 2011;3.
- [23] Lee MG, Yarranton GT. Inducible DNA repair in *Ustilago maydis*. *Mol Gen Genet* 1982;185(2):245–50.
- [24] Li H, Durbin R. Fast and accurate short read alignment with Burrows-Wheeler transform. *Bioinformatics* 2009;25(14):1754–60.
- [25] Liu Yi, Kim E, Li J, Kang M, Bentley WE, Payne GF. Electrochemistry for bio-device molecular communication: the potential to characterize, analyze and actuate biological systems. *Nano Commun Networks* 2017;11:76–89.
- [26] Llewellyn CA, Ains RL, Farnham G, Greig C. Synthesis, regulation and degradation of carotenoids under low level UV-B radiation in the filamentous Cyanobacterium *Chlorogloeopsis fritschii* PCC 6912. *Front Microbiol* 2020;11.
- [27] Malo ME, Bryan RA, Shuryak I, Dadachova E. Morphological changes in melanized and non-melanized *Cryptococcus neoformans* cells post exposure to sparsely and densely ionizing radiation demonstrate protective effect of melanin. *Fungal Biol* 2018;122(6):449–56.
- [28] Malo ME, Dadachova E. Melanin as an energy transducer and a radioprotector in black fungi. In: Tiquia-Arashiro SM, Grube M, editors. *Fungi in Extreme Environments: Ecological Role and Biotechnological Significance*. Cham: Springer International Publishing; 2019. p. 175–84.
- [29] Malo ME, Frank C, Dadachova E. Assessing melanin capabilities in radiation shielding and radioadaptation. *J Med Imag Radiat Sci* 2019;50(1):S2.
- [30] Malo ME, Frank C, Dadachova E. Radioadapted *Wangiella dermatitidis* senses radiation in its environment in a melanin-dependent fashion. *Fungal Biol* 2020;124(5):368–75.
- [31] Manning PL, Edwards NP, Bergmann U, Anné J, Sellers WI, van Veelen A, et al. Pheomelanin pigment remnants mapped in fossils of an extinct mammal. *Nat Commun* 2019;10(1).
- [32] McKenna A, Hanna M, Banks E, Sivachenko A, Cibulskis K, Kernytzky A, et al. The Genome Analysis Toolkit: a MapReduce framework for analyzing next-generation DNA sequencing data. *Genome Res* 2010;20(9):1297–303.
- [33] VENNY. An interactive tool for comparing lists with Venn Diagrams. <https://bioinfogp.cnb.csic.es/tools/venny/index.html>.
- [34] Onofri S, Barreca D, Selbmann L, Isola D, Rabbow E, Horneck G, et al. Resistance of Antarctic black fungi and cryptoendolithic communities to simulated space and Martian conditions. *Stud Mycol* 2008;61:99–109.
- [35] Onofri S, de Vera J-P, Zucconi L, Selbmann L, Scalzi G, Venkateswaran KJ, et al. Survival of antarctic cryptoendolithic fungi in simulated martian conditions on board the international space station. *Astrobiology* 2015;15(12):1052–9.
- [36] Pacelli C, Bryan RA, Onofri S, Selbmann L, Shuryak I, Dadachova E. Melanin is effective in protecting fast and slow growing fungi from various types of ionizing radiation. *Environ Microbiol* 2017;19(4):1612–24.
- [37] Pacelli C, Selbmann L, Zucconi L, Coleine C, de Vera J-P, Rabbow E, et al. Responses of the black fungus *Aspergillus niger* to simulated mars and space conditions on rock analogs. *Astrobiology* 2019;19(2):209–20.
- [38] Patro R, Duggal G, Love MI, Irizarry RA, Kingsford C. Salmon provides fast and bias-aware quantification of transcript expression. *Nat Methods* 2017;14(4):417–9.
- [39] Priebe S, Kreisel C, Horn F, Guthke R, Linde J. FungiFun2: a comprehensive online resource for systematic analysis of gene lists from fungal species. *Bioinformatics (Oxford, England)* 2015;31(3):445–6.
- [40] Reis-Mansour MCPP, Cardoso-Rurr JS, Silva JVMA, de Souza GR, Cardoso VdS, Mansoldo FRP, et al. Carotenoids from UV-resistant Antarctic Microbacterium sp. LEMMJ01. *Sci Rep* 2019;9(1).
- [41] Robertson KL, Mostaghim A, Cuomo CA, Soto CM, Lebedev N, Bailey RF, Wang Z. Adaptation of the black yeast *Wangiella dermatitidis* to ionizing radiation: molecular and cellular mechanisms. *PLoS One* 2012;7.
- [42] Romsdahl J, Blachowicz A, Chiang AJ, Chiang Y-M, Masonjones S, Yaegashi J, et al. International Space Station conditions alter genomics, proteomics, and metabolomics in *Aspergillus nidulans*. *Appl Microbiol Biotechnol* 2019;103(3):1363–77.
- [43] Romsdahl J, Blachowicz A, Chiang AJ, Singh N, Stajich JE, Kalkum M, Venkateswaran K, Wang CCC. Characterization of *Aspergillus niger* isolated from the international space station. *mSystems* 2018;3.
- [44] Romsdahl J, Blachowicz A, Chiang YM, Venkateswaran K, Wang CCC. Metabolomic analysis of *Aspergillus niger* isolated from the international space station reveals enhanced production levels of the antioxidant pyranonigrin A. *Front Microbiol* 2020;11:931.
- [45] Schultzhau Z, Chen A, Shuryak I, Wang Z. The Transcriptomic and Phenotypic Response of the Melanized Yeast *Exophiala Dermatitidis* to Ionizing Particle Exposure. *Research Square*; 2020.
- [46] Selbmann L, Zucconi L, Isola D, Onofri S. Rock black fungi: excellence in the extremes, from the Antarctic to space. *Curr Genet* 2015;61(3):335–45.
- [47] Shuryak I. Review of microbial resistance to chronic ionizing radiation exposure under environmental conditions. *J Environ Radioact* 2019;196:50–63.
- [48] Tugay T, Zhdanova NN, Zheltonozhsky V, Sadovnikov L, Dighton J. The influence of ionizing radiation on spore germination and emergent hyphal growth response reactions of microfungi. *Mycologia* 2006;98(4):521–7.
- [49] Tugay TI, Zheltonozhskaya MV, Sadovnikov LV, Tugay AV, Farfan EB. Effects of ionizing radiation on the antioxidant system of microscopic fungi with radioadaptive properties found in the Chernobyl exclusion zone. *Health Phys* 2011;101(4):375–82.
- [50] Turick CE, Ekechukwu AA, Milliken CE, Casadevall A, Dadachova E. Gamma radiation interacts with melanin to alter its oxidation-reduction potential and results in electric current production. *Bioelectrochemistry* 2011;82(1):69–73.
- [51] Verma NC, Singh RK. Stress-inducible DNA repair in *Saccharomyces cerevisiae*. *J Environ Pathol Toxicol Oncol* 2001;20(1):7.
- [52] Wahba A, Rath BH, Bisht K, Camphausen K, Tofilon PJ. Polysome profiling links translational control to the radioresponse of glioblastoma stem-like cells. *Cancer Res* 2016;76(10):3078–87.
- [53] Warner JR. The economics of ribosome biosynthesis in yeast. *Trends Biochem Sci* 1999;24(11):437–40.
- [54] Warris A, Ballou ER. Oxidative responses and fungal infection biology. *Semin Cell Dev Biol* 2019;89:34–46.
- [55] Zhang F, Kearns SL, Orr PJ, Benton MJ, Zhou Z, Johnson D, et al. Fossilized melanosomes and the colour of Cretaceous dinosaurs and birds. *Nature* 2010;463(7284):1075–8.
- [56] Zhdanova NN, Tugay T, Dighton J, Zheltonozhsky V, Mcdermott P. Ionizing radiation attracts soil fungi. *Mycol Res* 2004;108(9):1089–96.